Article

A Sialic Acid-Caged Generic Platform for Sialoengineering of Tumors with Artificial Immuno-Ligand

Shuo Zhang [1,†], Huiling Dong [2,†], Shixiong Wen [3,4], Zejing Lin [1], Xuanjun Wu [2,*], Jiahuai Han [3,4,*], and Shoufa Han [1,3,*]

[1] State Key Laboratory for Physical Chemistry of Solid Surfaces, Department of Chemical Biology, College of Chemistry and Chemical Engineering, the Key Laboratory for Chemical Biology of Fujian Province, and The MOE Key Laboratory of Spectrochemical Analysis & Instrumentation, Xiamen University, Xiamen 361005, China
[2] National Glycoengineering Research Center, Shandong Key Laboratory of Carbohydrate Chemistry and Glycobiology, NMPA Key Laboratory for Quality Research and Evaluation of Carbohydrate-Based Medicine, Shandong University, Qingdao 266237, China
[3] Academician Workstation of Immune Cell Signal Transduction, School of Basic Medicine, Chongqing Medical University, Chongqing 400016, China
[4] State Key Laboratory of Cellular Stress Biology, School of Life Science Xiamen University, Xiamen 361005, China
* Correspondence: xuanjun@sdu.edu.cn (X.W.); jhan@xmu.edu.cn (J.H.); shoufa@xmu.edu.cn (S.H.)
† These authors contributed equally to this work.
Received: 16 June 2025; Revised: 27 June 2025; Accepted: 4 July 2025; Published: 30 July 2025

Abstract: Selective glycoengineering of tumors in vivo is a highly promising strategy for tumor treatment. Although metabolic glycan labeling using precursors of sialic acid (Sia) is an effective method for attaching chemical probes to cell surfaces, it often lacks specificity for tumors. Herein, we report a tumor-activated sialoengineering approach utilizing Sia with C1-carboxylate caged with lysine (K). Probe decaging by carboxypeptidase in tumors enables tumor-exofacial expression of abiotic Sia tolerating differing C9-substitutions such as azide (^{Az}Sia) and *m*-phenoxybenzamide (^{PBA}Sia). Notably, ^{PBA}Sia acts as a high-affinity ligand for the CD22 receptor of B cells. Treatment with ^{PBA}Sia-K leads to robust suppression of subcutaneous B16-F10 tumors in mice. These data show the potential of C1-caged Sia to function as a generic small-molecule platform for in vivo sialoengineering of tumor cells, allowing for the generation of cell surface-anchored C9-substituted Sia that could be harnessed to stimulate an anti-tumor response.

Keywords: metabolic engineering; sialylation; decaging; CD22 high-affinity ligand; tumor suppression

1. Introduction

Small-molecule probes capable of inducing an anti-tumor response but sparing normal cells are valuable for therapeutic purposes. The conjugation of therapeutic agents with small-molecule natural ligands like folate and biotin has proven effective in treating tumors via binding to specific receptors. However, the selectivity of self-receptor-targeted therapy can be compromised by the presence of these receptors on off-target cell types or healthy tissues, albeit at lower abundance [1]. Cell surface receptor-ligand interactions play a fundamental role in determining cell fate [2]. Cancer cells can escape immune surveillance, reflecting insufficiency of native receptor-ligand pairs between cancer and immune cells to mount antitumor immunity. The advances in the development of artificial ligands have created opportunities to manipulate biological receptors [3,4], thus in vivo decoration of tumor cell surface with small-molecule artificial ligands holds the potential to reprogram tumor-immune cell interplay.

Mammalian cells are enveloped with a dense layer of glycans, which are often terminated with sialic acid (Sia), a 9-carbon monosaccharide featuring a carboxylic acid at C1 position [5]. By exploiting the substrate promiscuity of sialylation pathway, metabolic glycoengineering (MGE) allows incorporation of unnatural Sia onto cell surface through feeding cells with metabolic precursors of Sia such as *N*-azidoacetyl mannosamine [6–15]. These abiotic precursors are enzymatically converted to cognate C5 *N*-acyl Sia that permeates sialylation pathway and then is incorporated into diverse glycoconjugates destined for ecto-plasma. The resultant C5 *N*-acyl-modified Sia expressed on cell surface provides a bioorthogonal handle for metabolic glycan labeling [7,16]. However, because the Sia biosynthetic pathway is present in diverse cell types and conventional azidosugars lack cell-type

specificity, additional mechanisms are warranted to achieve cell- or tissue-specific MGE [17–22]. One promising approach involves using *N*-acyl mannosamines chemically caged at C1 or C6 hydroxyl group [23–26]. The decaging of these molecules by biomarkers like enzymes releases *N*-acyl mannosamines, initiating MGE of the host cells (Scheme 1A). Phosphorylation of C6 hydroxyl group of *N*-acyl mannosamines is an essential step in biosynthetic transforming them to cognate C5 *N*-acyl Sia (Scheme 1A). Thus precursor-based MGE mechanistically yields N-acyl-modified Sia with an intact C9 hydroxyl group incorporated on cell surface, as dictated by the sialylation metabolic machinery. Therefore C9-substituted Sia is inapplicable to sialoenginnering via current precursor-based approaches.

Sialosides with nominated C9 substitutions serve as high-affinity ligands of Siglecs, a family of Sia-binding lectins restricted to immune cells. For instance, CD22 on B cells binds avidly with ^{PBA}Siaα2,6gal as compared to its natural ligand Siaα2,6gal [27,28]. Furthermore, immunotherapy of B-cell lymphoma has been reported through the adoptive transfer of ^{PBA}Sia-modified natural killer (NK) cells into mice [29]. This suggests the applicability of CD22-^{PBA}Sia pair to boost B-cell interaction with ^{PBA}Sia-expressing cells in vivo. On the basis of these findings and as several B-cell subsets are important players in anti-tumor immunity, we sought to explore the potential of C9-modified Sia, such as ^{PBA}Sia, in modulating tumor growth by exploiting the interaction between cancer cells and B cells. We thus employed C1-caged Sia with C9 substitutions for tumor-specific MGE and tumor suppression in mice (Scheme 1B), with the goal of investigating the therapeutic potential of this approach in altering tumor growth.

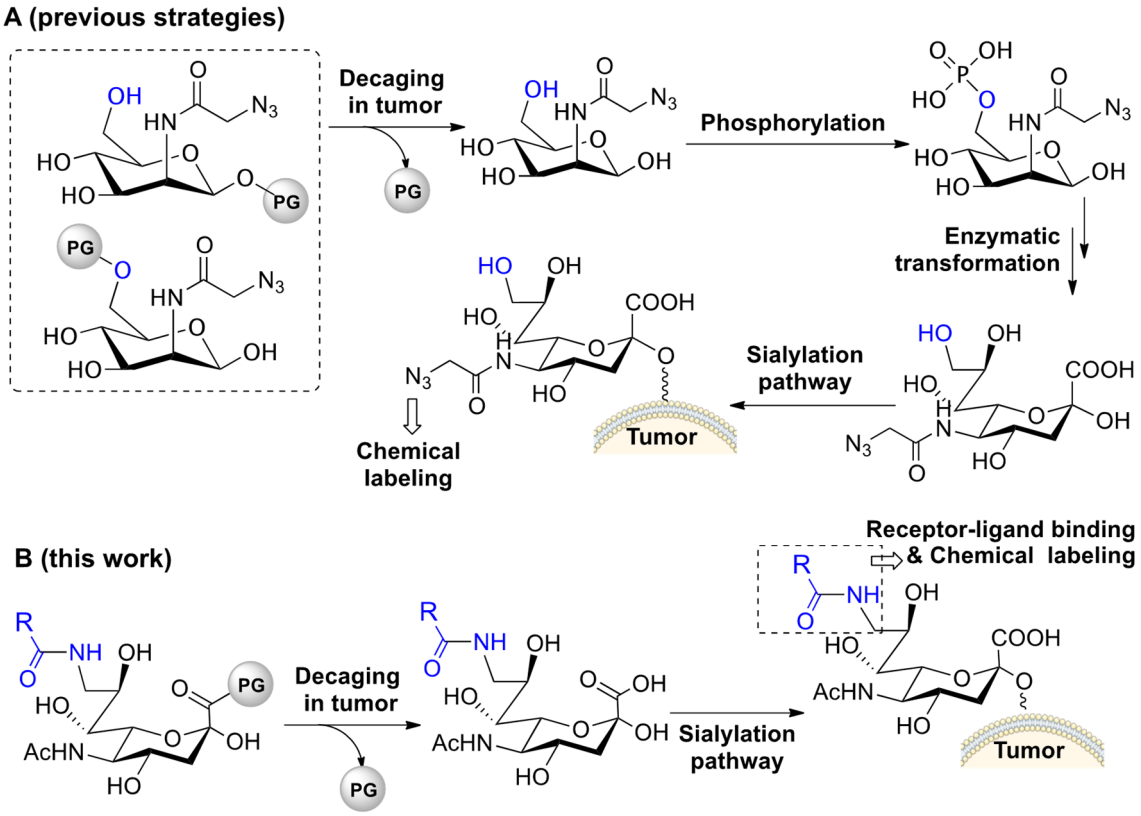

Scheme 1. Overview of tumor-specific MGE with C1-caged Sia. (**A**) Previously reported tumor-targeted MGE with caged *N*-azidoacetyl mannosamines. This method operates through a multi-step process that relies stringently on the decaging of probes within tumor cells as well as phosphorylation of C6 hydroxyl group of *N*-acyl mannosamine. This approach restricts the expression on the cell surface to C5 *N*-acyl Sia with C9 OH. (**B**) Proposed tumor-specific MGE using C9-substituted Sia caged at C1. The enzymatic decaging process releases C9-modified Sia, which is later attached to the tumor cell surface, resulting in a high-affinity ligand of CD22 of B cells.

2. Results and Discussion

2.1. Design of C-1-Caged Sia for Enzyme-Triggered Sialoengineering with C9-Substituted Sia

In addition to the commonly used *N*-acyl mannosamines for MGE, C9-substituted Sia could be taken up by cells and metabolically integrated into cell surface glycans [30,31]. Considering that carboxypeptidases cleave C-terminal amino acids from peptides to influence specific cancers [32,33], we aimed to cage C1 carboxylic acid of

Sia with amino acids for enzyme-triggered MGE in tumor cells. We synthesized ^{Az}Sia-E, ^{Az}Sia-F, and ^{Az}Sia-K by amidation of 9-azido-Sia (^{Az}Sia) with the amino acids glutamate (E), phenylalanine (F), and lysine (K), representing anionic, neutral, and cationic side chains, respectively (refer to Scheme S1, Supporting Information).

We initially cultured a panel of cell lines with ^{Az}Sia and subsequently treated these cells with fluorescein isocyanate-conjugated DBCO (^{DBCO}FITC), which is impermeable to the cell plasma membrane due to its hydrophilic nature. This allows fluorescence labeling of ^{Az}Sia on the cell surface through stain-promoted azide-alkyne cyclization (SPAAC) (Figure 1A). The resulting fluorescence on the cell surface served as a measure of MGE. Relative to control cells lacking sugar, ^{Az}Sia generated strong green fluorescence across all tested cell lines including A549 (a human lung adenocarcinoma cell line), B16-F10 (a murine skin melanoma cell line), MCF-7 (a breast cancer cell line), HeLa (a cervical cancer cell line), PC3 cells (a cell line of prostatic small cell carcinoma) and RAW 264.7 (a noncancerous murine macrophage cell line) (Figure 1B). Following verification of an effective sialylaiton pathway in these cell lines, we tested chemically caged Sia for MGE by feeding ^{Az}Sia-E, ^{Az}Sia-F or ^{Az}Sia-K to these cancer cell lines (Figure 2A). Subsequent cell staining with ^{DBCO}FITC reveals that those treated with ^{Az}Sia-E or ^{Az}Sia-F exhibited dim and sparse fluorescence, similar to ^{Az}Sia-free cells (Figure 2B), demonstrating invalid MGE in these cell lines. This lack of MGE with ^{Az}Sia-E and ^{Az}Sia-F indicates that the caging of the C1 carboxylate of Sia effectively prevents non-specific MGE. Encouragingly, treatment with ^{Az}Sia-K led to bright fluorescence on the plasma membrane of B16-F10, MCF-7, HeLa, and RAW264.7, but A549 and PC3 cells did not exhibit similar results (Figure 2B). This variability demonstrates that the decaging of ^{Az}Sia-K and subsequent MGE are dependent on the specific cell type.

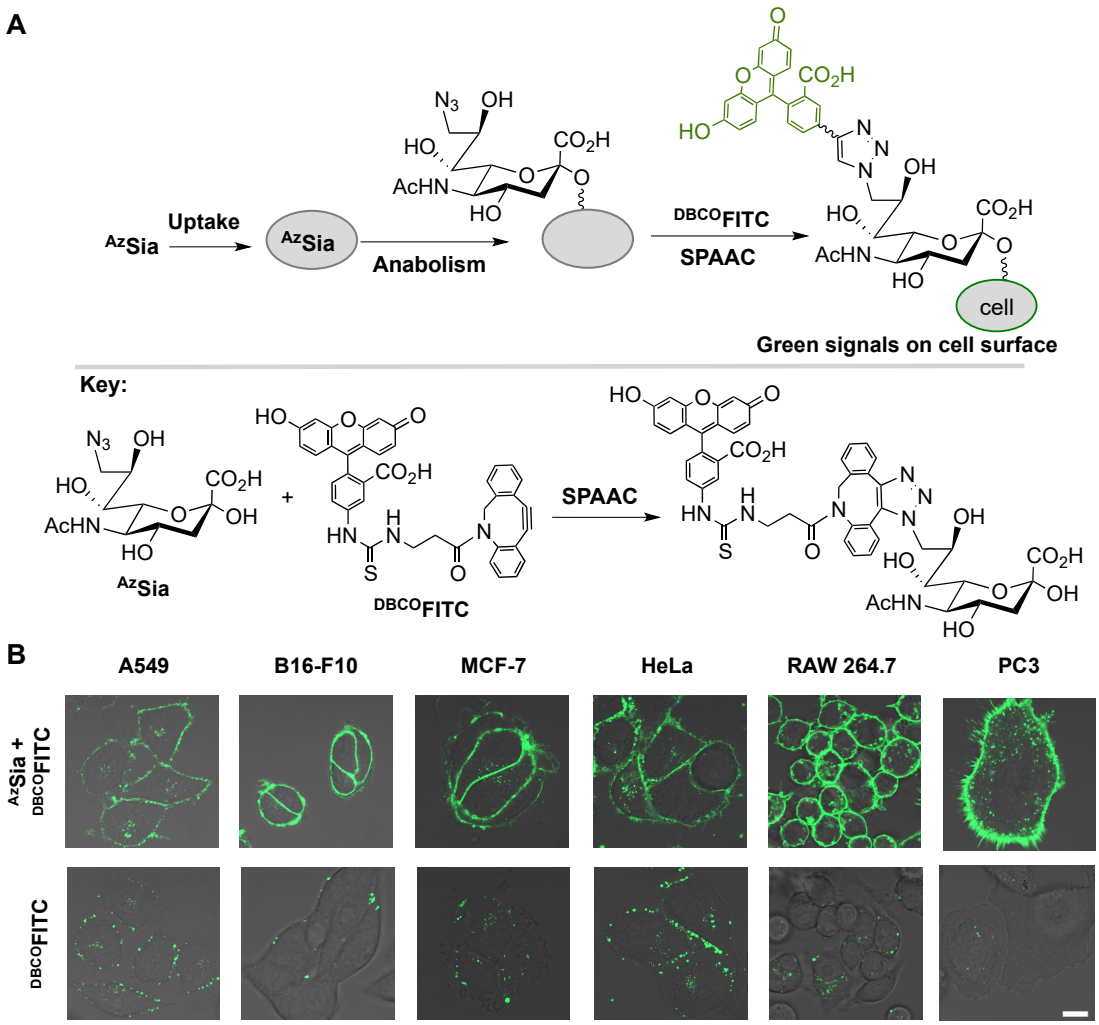

Figure 1. Ubiquitous MGE with ^{Az}Sia in different cell lines. (**A**) Illustration for incorporation of ^{Az}Sia onto the cell surface and fluorescence tagging of ^{Az}Sia with ^{DBCO}FITC. The key shows chemical structures of ^{Az}Sia and ^{DBCO}FITC, as well as ligation of ^{DBCO}FITC to ^{Az}Sia via SPAAC. (**B**) Expression of ^{Az}Sia on the cell surface. A549, B16-F10, MCF-7, HeLa, RAW 264.7, and PC3 cells were cultivated in Dulbecco's modified Eagle medium (DMEM) spiked with ^{Az}Sia or no addition for 24 h, respectively, washed with PBS, and then stained with ^{DBCO}FITC (50 μM, 2 h) before confocal microscopic analysis. Scale bar: 10 μm.

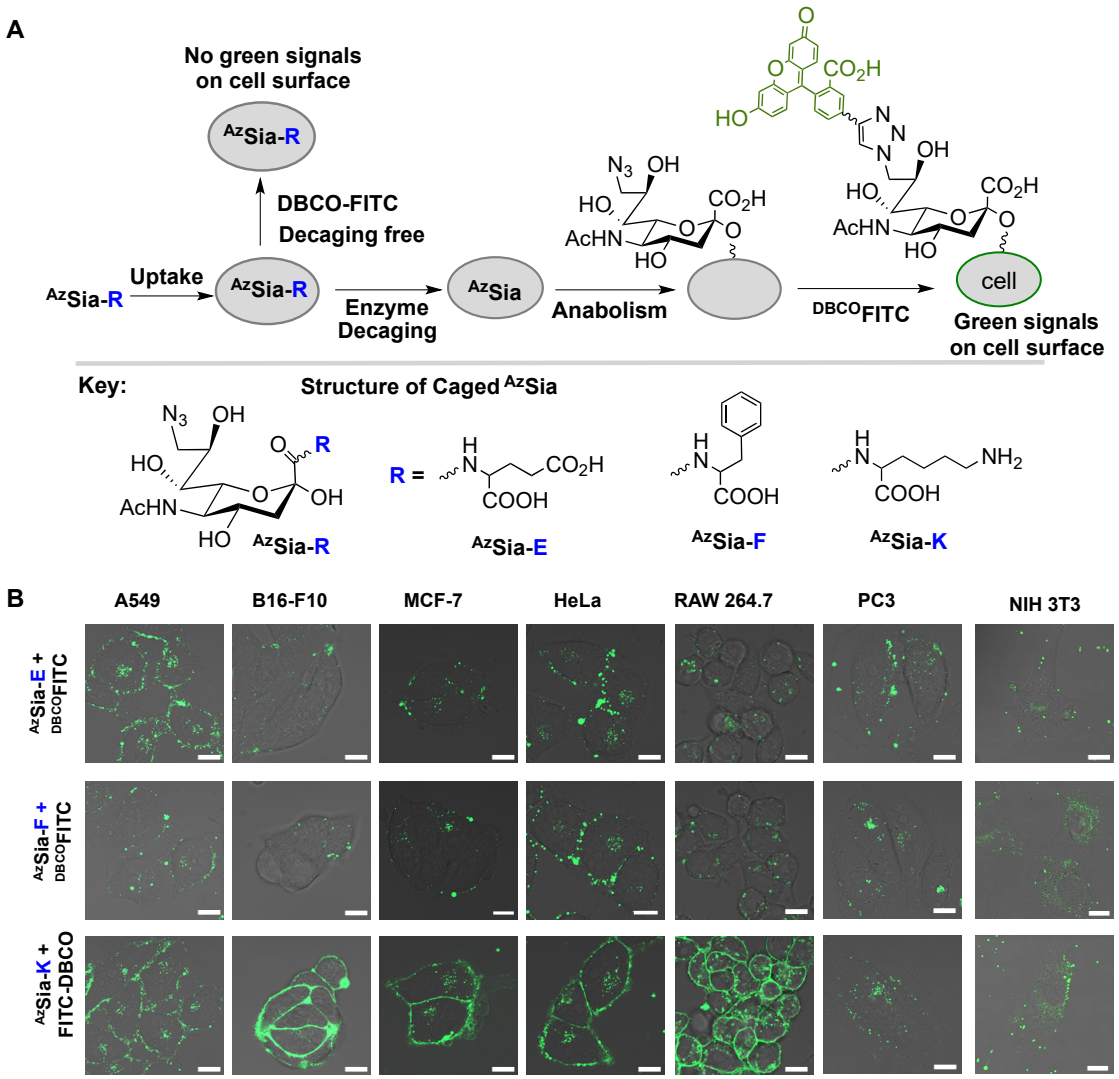

Figure 2. Cell type-dependent MGE with C1-masked ^{Az}Sia. (**A**) Decaging-conferred cell surface labeling with ^{DBCO}FITC. Decaging of C1-masked ^{Az}Sia in cells allows MGE and fluorescence labeling of cell surface. The lack of decaging maintains the sugar in caged state, preventing expression of ^{Az}Sia on cell surface, as evident from invalid fluorescence labeling. The key shows chemical structures of ^{Az}Sia-E, ^{Az}Sia-F and ^{Az}Sia-K. (**B**) Cell type-specific MGE with ^{Az}Sia-K over ^{Az}Sia-E and ^{Az}Sia-F. A549, B16-F10, MCF-7, HeLa, RAW 264.7, PC3 and NIH 3T3 were cultivated in DMEM spiked with ^{Az}Sia-E, ^{Az}Sia-F, ^{Az}Sia-K or no addition for 24 h, respectively. After washing with PBS, and staining with ^{DBCO}FITC, the cells were imaged by confocal fluorescence microscopy. Scale bars: 10 μm.

2.2. In Vitro Metabolic Glycan Engineering with C1-Caged C9-Substituted Sia

Carboxypeptidase B hydrolyzes C-terminal basic amino acids such as lysine from substrates. To ascertain enzymatic decaging of ^{Az}Sia-K, in vitro hydrolysis of ^{Az}Sia-K was tested in an aqueous solution containing carboxypeptidase B. LC-MS analysis of the assay solution revealed formation of at peak corresponding to ^{Az}Sia (molecular weight found 333.1048; calculated 333.1052) (ESI, Figure S1). This demonstrates the capability of carboxypeptidase B to decage ^{Az}Sia-K by hydrolytic removal of lysine at C1. To confirm the involvement of the carboxypeptidase B in the observed MGE, B16-F10 cells were fed ^{Az}Sia-K in combination with 2-guanidinoethylmercapto-succinic acid (GEMSA), a potent inhibitor of carboxypeptidase B. GEMSA significantly decreased exofacial green fluorescence in cells cultured with ^{Az}Sia-K as compared to GEMSA-free counterparts (ESI, Figure S2). In addition, Western blotting analysis confirmed the expression of carboxypeptidase B in B16-F10 cells but not in A549 cells (ESI, Figure S3). Combined, these data support carboxypeptidase decaging conferred MGE with ^{Az}Sia-K in B16-F10 cells.

CD22 is a B cell-restricted Sia-binding immunoglobulin-like lectin capable of inhibiting B cell receptor signaling. To date, CD22 has evolved into a promising target for the treatment of B lymphoma and leukemia [34–38]. However, the use of CD22 expressed on healthy B cells in the treatment of malignant cells has been largely

unexplored. B cells comprise functionally distinct subsets that exert both pro- and anti-tumor immune responses [39–42]. We hypothesized that glyco-editing of malignant cells with a high-affinity ligand of CD22, such as ^{PBA}Sia, could boost B-cell interaction with glyco-edited cells. This potentially provides a small-molecule-based approach for in vivo immunomodulation. Given the bulkier size of *m*-phenoxybenzoyamido (PBA) group compared to the azido group, we sought to determine whether ^{PBA}Sia could be incorporated into glycocalyx by MGE. ^{PBA}Sia on the cell surface is chemically inert for classical bioorthogonal fluorescence labeling. To address this, we synthesized the proxy C9-*m*-(4-azidophenoxy)benzamido-Sia (^{AzPBA}Sia) to elucidate its compatibility with MGE (Figure 3A; ESI, Scheme S2†). B16-F10 and HeLa cells were cultivated with ^{AzPBA}Sia, followed by staining with ^{DBCO}FITC. Bright green signals were identified on the plasma surface of both cell lines treated with ^{AzPBA}Sia but not sugar-free control cells (Figure 3B), demonstrating MGE-mediated incorporation of ^{AzPBA}Sia into the cell surface glycocalyx and the applicability of ^{PBA}Sia for MGE.

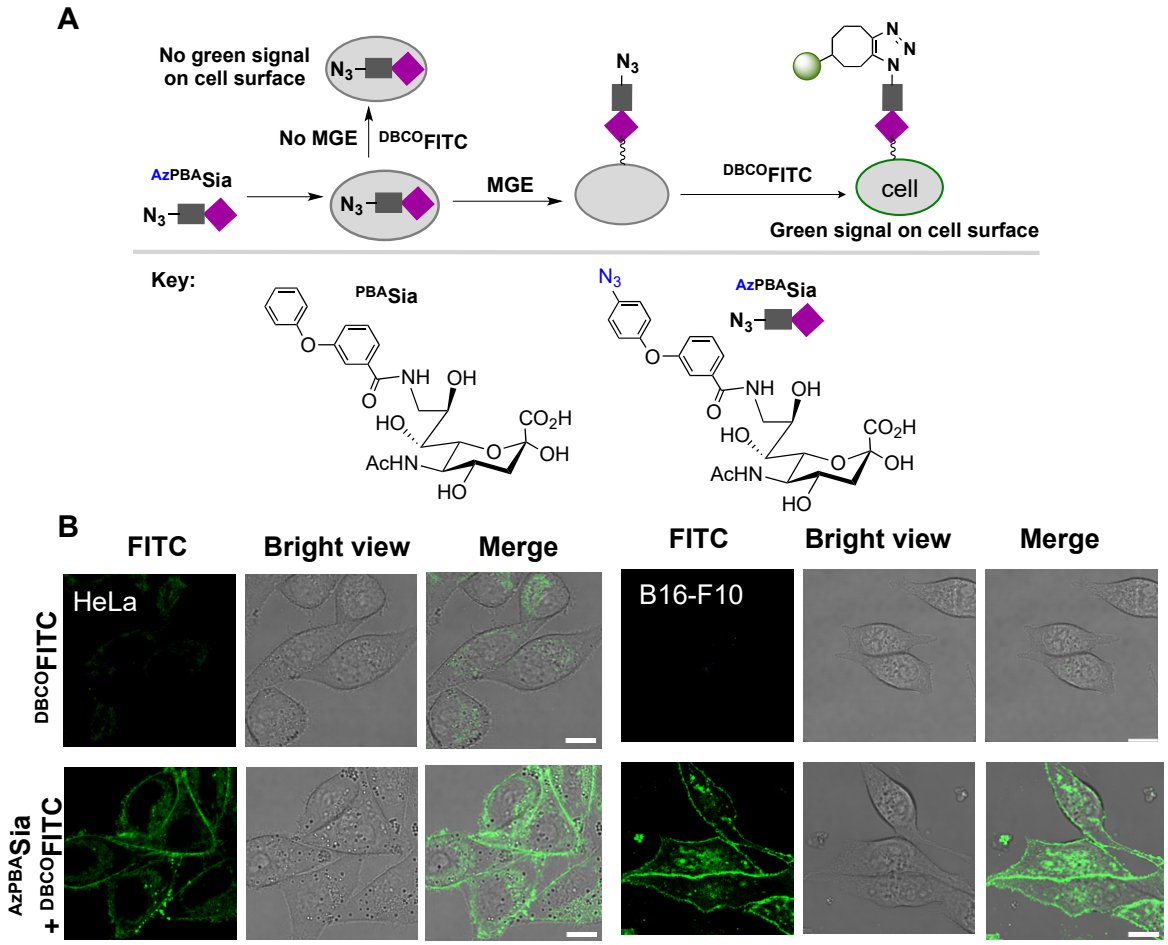

Figure 3. Compatibility of ^{AzPBA}Sia with MGE. (**A**) Schematic illustration for fluorescence labeling of ^{AzPBA}Sia displayed on the cell surface. MGE utilizing ^{AzPBA}Sia results in the exposure of azido moiety on the cell surface, which can be detected through fluorescence labeling. Lack of cell surface-associated fluorescence indicates a failed MGE due to ^{AzPBA}Sia's inability to infiltrate the sialylation pathway. The accompanying key shows chemical structures of ^{PBA}Sia and ^{AzPBA}Sia. (**B**) Metabolic incorporation of ^{AzPBA}Sia on the cell surface. B16-F10 and HeLa cells were cultivated in DMEM containing ^{AzPBA}Sia or no addition for 24 h. The cells were washed with PBS, stained with ^{DBCO}FITC, and then visualized using confocal fluorescence microscopy. Scale bars: 10 μm.

2.3. In Vivo Effect of C1-Caged C9-Sustituted Sia on Tumor Growth

Melanoma is a highly aggressive form of skin cancer associated with significant mortality rates. The B16-F10 cell line, a widely used model of human melanoma, exhibits hypersialylation [43], reflecting active sialylation in vivo. Notably, B16-F10 cells expressed a high level of the Siaα2,6gal epitope [44]. These characteristics are vital for the anticipated tumor-B cell interaction conferred by MGE with ^{PBA}Sia. Therefore, we selected B16-F10 tumors to assess the impact of ^{PBA}Sia-K on tumor progression in mice.

We also aimed to enhance antitumor effects by integrating pharmacological agents with caged Sia. Consequently, ^{PBA}Sia-K was butyrated at C2/4/7/8 hydroxyl positions to create ^{PBA}Sia-Bu-K (Figure 4A; ESI, Scheme S3†). The rationale to test ^{PBA}Sia-Bu-K was two-fold. First, *O*-butyration increases the hydrophobicity of the probe, as ^{PBA}Sia-K is highly hydrophilic. Second, hydrolysis of ^{PBA}Sia-Bu-K in tumor cells by esterases releases butyrate, a short-chain fatty acid with inhibitory effects on certain cancers [45–48]. Additionally, since Sia with a biphenyl carboxylic group (BPC) at C9 (^{BPC}Sia) serves as an affinity ligand of CD22 [49–51], ^{BPC}Sia-Bu-K was synthesized to explore the differing effects of CD22 ligands on tumor growth (Scheme S3, Supporting Information).

Before investigating the in vivo effect of caged Sia on tumors, we first examined ^{PBA}Sia-K, ^{PBA}Sia-Bu-K and ^{BPC}Sia-Bu-K for in vitro cytotoxicity on B16-F10 cells. ^{PBA}Sia-K and ^{PBA}Sia-Bu-K gave no obvious reduction in viability of B16-F10 cells at probe concentrations up to 200 μM, whereas ^{BPC}Sia-Bu-K caused a 30% decrease in cell viability (ESI, Figure S4A). Moreover, these caged Sia gave no apparent inhibition on the proliferation of B16-F10 cells in vitro after 5-day culturing (ESI, Figure S4B). To assess the antitumor effect of caged Sia, B16-F10 cells were subcutaneously injected into C57BL/6 mice. When the tumor foci reached 80-100 mm^3, mice were subjected to tail-vein injection with phosphate-buffered saline (PBS), ^{PBA}Sia-K, ^{PBA}Sia-Bu-K or ^{BPC}Sia-Bu-K at 11.0 or 33.0 μmol kg^{-1} (referred to as high or low dose group) on the 7th, 9th, and 11th day post tumor cell inoculation.

The mice were monitored for changes in body weight and tumor volume. No signs of abnormal behavior were observed following the administration of caged Sia. A moderate-to-slight increase in body weight was noted in mice receiving PBS, ^{BPC}Sia-Bu-K or a low dose of ^{PBA}Sia-Bu-K up to 14th day post-tumor cell inoculation (the endpoint), whereas the body weight of mice with a high dose of ^{PBA}Sia-Bu-K remained largely unaltered (Figure 4B, ESI, Figure S5). Higher doses of ^{PBA}Sia-Bu-K or ^{BPC}Sia-Bu-K resulted in greater suppression of tumor volume (Figure 4C, ESI, Figure S5). Compared to PBS group, ^{PBA}Sia-Bu-K and ^{BPC}Sia-Bu-K (33.0 μmol kg^{-1}) elicited reductions in tumor volume of 80% and 50%, respectively, at the endpoint (Figure 4C), demonstrating the superiority of ^{PBA}Sia-Bu-K in suppressing B16-F10 tumor growth in vivo. Furthermore, ^{PBA}Sia-Bu-K caused a 2-fold greater reduction in tumor volume compared to ^{PBA}Sia-K (Figure 4C), showing that O-butyration benefits tumor suppression. This finding supports the use of the C2/4/7/8 hydroxyl group of caged Sia in combination with pharmacological agents to potentiate MGE-based immunotherapy. At 14th day post-injection of B16-F10 cells, the tumors were excised and weighed, confirming the inhibition order of ^{PBA}Sia-Bu-K > ^{BPA}Sia-Bu-K > ^{PBA}Sia-K > PBS (Figure 4D,E; Figure S5D,E, Supporting Information). Since caged ^{PBA}Sia exhibited no obvious inhibition of proliferation and viability of B16-F10 cells in vitro *(*ESI, Figure S4**)**, the marked retardation of B16-F10 tumor growth caused by ^{PBA}Sia-K and ^{PBA}Sia-Bu-K could be ascribed to MGE-mediated cell surface expression of ^{PBA}Sia that enhances tumor interaction with B cells.

With CD22-ligand conferred tumor suppression, we explored the possible involvement of B cells by measuring intratumoral B cell abundance. Tumors from mice injected with ^{PBA}Sia-Bu-K or PBS were harvested and homogenized. The resultant cell sample was stained with FITC-labeled anti-CD19 antibody and then analyzed by flow cytometry. This revealed that the mean fluorescence intensity was three-fold brighter on cells from ^{PBA}Sia-Bu-K-treated tumor than on those derived from PBS-treated tumor (ESI, Figure S6). As CD19 is a transmembrane glycoprotein specific for B cells, this finding confirm that $CD19^+$ B cells are enriched in ^{PBA}Sia-Bu-K-treated tumors, thus confirming engagement of B cells in ^{PBA}Sia-mediated immunosuppression.

Sia-Siglec axis functions as a critical immune checkpoint. Sia overexpressed on malignant cells benefits immune evasion [52–54]; whereby Sia binding in trans with Siglec has been documented to dampen immunoreactivity of Siglec-expressing immune cells [55,56]. Interestingly, our results on ^{PBA}Sia-conferred tumor suppression clearly show antitumor effects of enriched intratumoral B cells, although the mechanism remains to be defined. To date, much effort has been devoted to bifunctional affinity probes that act by binding to tumor surface biomarkers with one end and antibody or immune cells on the other [57–60]. Complementing this tripartite approach, we employ decaging-mediated MGE to covalently attach affinity ligands on the tumor surface to elicit ligand-receptor interaction and antitumor immunity. Without the need for meticulous optimization on tripartite tumor-bifunctional ligand-antibody/immune cell complex, our approach offers a simplified bipartite approach to modulate tumor-immune cell interaction.

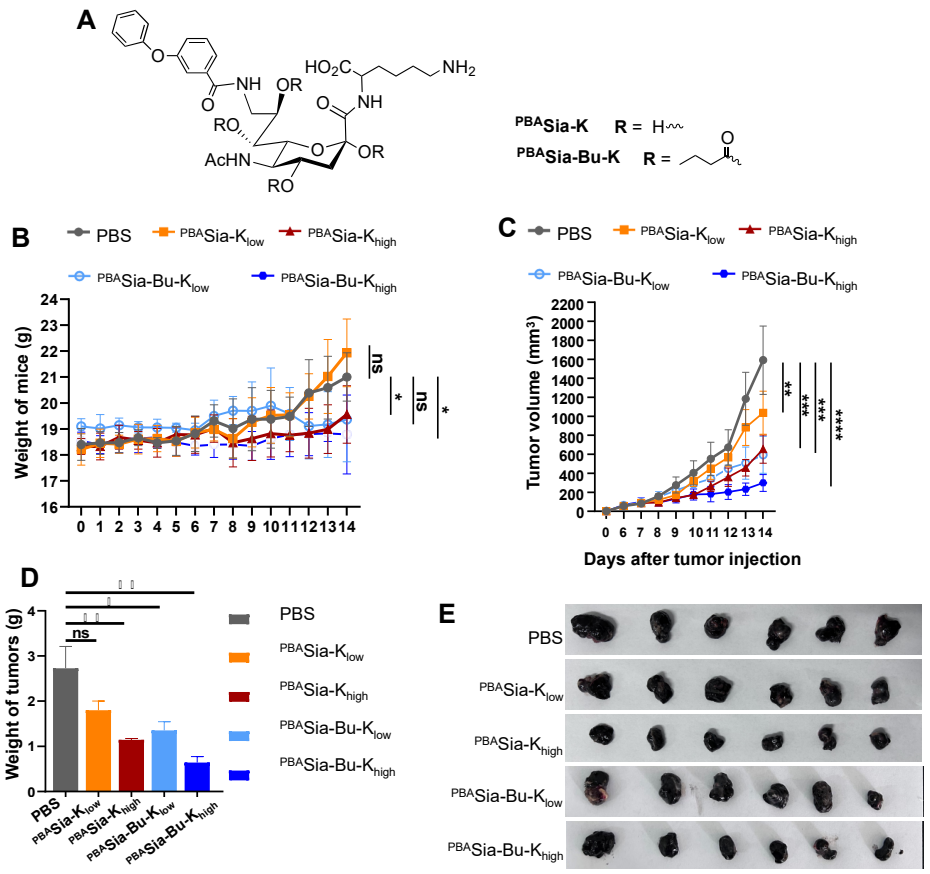

Figure 4. Evaluation of in vivo anticancer efficiency of caged ^{PBA}Sia. (**A**) Chemical structure of ^{PBA}Sia-K, ^{PBA}Sia-Bu-K, and ^{BPC}Sia-Bu-K. Temporal changes in body weight (**B**) and tumor volume (**C**) of mice injected with caged Sia. C57BL/6 mice subcutaneously inoculated with B16-F10 cells were treated with tail-vein injection of PBS (100 μL), ^{PBA}Sia-K (11.0 or 33.0 μmol kg^{-1}), ^{PBA}Sia-Bu-K (11.0 or 33.0 μmol kg^{-1}) or ^{PBA}Sia-Bu-K (11.0 or 33.0 μmol kg^{-1}). The tumors were excised on the 14th day after probe injection, measured for mass (**D**), and pictured (**E**). Tumor weight and volume were quantified by GraphPad Prism 8 software. Data were presented as means ± SEM of a representative assay. n = 6. ns, non-significant; * $p \leq 0.05$, ** $p \leq < 0.01$, *** $p < 0.001$, **** $p < 0.0001$ (*t*-test).

3. Conclusions

Tumor-specific sialoengineering is a highly promising strategy for immunomodulation. One method to selective tumor sialoengineering involves using caged Sia precursors. However, this method leads to expression of *N*-acyl Sia with intact C9 hydroxyl group due to inherent metabolic constraints. We thus designed C1-caged Sia for in vivo glyco-editing of tumor cells with C9-substituted Sia (^{PBA}Sia), the high-affinity ligand for CD22 of B cells. Our results demonstrate that decaging of ^{PBA}Sia-K triggered tumor sialoengineering and effective suppression of B16-F10 tumors in a murine model. Unlike immunotherapy strategies that involve genetic or biochemical modification of immune cells *ex vivo* for tumor targeting [61], our method relies solely on the intravenous injection of caged ^{PBA}Sia, which culminates in tumor surface expression of ^{PBA}Sia, whereby acting to promote B cell-tumor interaction. This straightforward approach provides an accessible and effective tool for modulating anti-tumor immunity in vivo, and presents opportunities for further enhancement by incorporating alternative caging moieties at C1 or introducing artificial ligands or antigens at C9, either individually or in synergy. In summary, this study demonstrates that C1-caged Sia may serve as a versatile platform for tumor-specific sialoengineering with C9-functionalized Sia, offering a potential tool to manipulate the Sialic acid-Siglec axis in vivo.

Supplementary Materials: The following supporting information can be downloaded at: https://media.sciltp.com/articles/others/250 7291731529709/SupportingInformation-HM-updated-2.pdf, Scheme S1-S3: Synthetic routes for C-1-caged Sia and its precursors. Figure S1: Carboxypeptidase B-catalysis triggered formation of ^{Az}Sia from ^{Az}Sia-K. Figure S2: carboxypeptidase B-dependent MGE with Caged Sia. Figure S3: Western Blotting analysis on carboxypeptidase B in B16-F10 cells. Figure S4: In vitro effects of C1-caged Sia on B16-F10 cells. Figure S5: Evaluation of in vivo antitumor efficiency of caged ^{BPC}Sia. Figure S6: Evaluation on B cell levels in

B16-F10 tumors. Figures S7–S38: $^{1}H/^{13}C$-NMR and Mass spectra of caged Sia and its precursors. Reference [62] are cited in the supplementary materials.

Author Contributions: S.Z. and Z.L.: synthesis and in vitro analysis of chemically caged Sia. S.W.: analysis of C-1-caged Sia in cells; H.D.: tumor suppression in mice. S.H.: concept of C-1-caged Sia for tumor glcoengineering. S.H., J.H. and X.W.: supervision, manuscript writing and editing. All authors have read and agreed to the published version of the manuscript.

Funding: This research was funded by the Fundamental Research Funds for the Central Universities, grant number 20720240126; National Science Foundation of China, grant number 22177096, 82388201, 22377065; the National Key R&D Program of China, grant number 2020YFA0803500, the CAMS Innovation Fund for Medical Sciences , grant number 2019-I2M-5-062, the Fujian Province Central to Local Science and Technology Development Special Program, grant number 2022L3079, the Fu-Xia-Quan Zi-Chuang District Cooperation Program, grant number 3502ZCQXT2022003; the Excellent Youth Fund Project supported by Shandong Provincial Natural Science Foundation, grant number ZR2022YQ17; and the Taishan Scholars Program for Young Experts of Shandong Province, grant number tsqn202312047.

Institutional Review Board Statement: The in vivo study on mice was conducted according to the guidelines of the Animal Care and Use Committee of Shandong University and approved by the Animal Ethics Committee of the College of Life Sciences at Shandong University (Approval No. SYDWLL-2023-037, approved on 25 February 2023).

Data Availability Statement: Online supporting Information available.

Acknowledgments: S. Han was supported by grants from NSF China (22177096), the Fundamental Research Funds for the Central Universities (20720240126); J. Han was supported by NSF China (82388201), the National Key R&D Program of China (2020YFA0803500), the CAMS Innovation Fund for Medical Sciences (2019-I2M-5-062), the Fujian Province Central to Local Science and Technology Development Special Program (2022L3079) and the Fu-Xia-Quan Zi-Chuang District Cooperation Program (3502ZCQXT2022003). X. Wu was supported by NSF China (22377065), the Excellent Youth Fund Project supported by Shandong Provincial Natural Science Foundation (ZR2022YQ17), and the Taishan Scholars Program for Young Experts of Shandong Province (No. tsqn202312047).

Conflicts of Interest: There are no conflict to declare.

References

1. Shmeeda, H.; Mak, L.; Tzemach, D.; Astrahan, P.; Tarshish, M.; Gabizon, A. Intracellular uptake and intracavitary targeting of folate-conjugated liposomes in a mouse lymphoma model with up-regulated folate receptors. *Mol. Cancer Ther.* **2006**, *5*, 818–824.
2. Rouault, H.; Hakim, V. Different cell fates from cell-cell interactions: Core architectures of two-cell bistable networks. *Biophys. J.* **2012**, *102*, 417–426.
3. Monge, P.; Søgaard, A.B.; Andersen, D.G.; Chandrawati, R.; Zelikin, A.N.. Synthetic chemical ligands and cognate antibodies for biorthogonal drug targeting and cell engineering. *Adv. Drug Deliv. Rev.* **2021**, *170*, 281–293.
4. Guryanov, I.; Fiorucci, S.; Tennikova, T. Receptor-ligand interactions: Advanced biomedical applications. *Mat. Sci. Eng. C* **2016**, *68*, 890–903.
5. Angata, T.; Varki, A. Chemical diversity in the sialic acids and related alpha-keto acids: An evolutionary perspective. *Chem. Rev.* **2002**, *102*, 439–469.
6. Prescher, J.A.; Dube, D.H.; Bertozzi, C.R. Chemical remodelling of cell surfaces in living animals. *Nature* **2004**, *430*, 873–877.
7. Wang, H.M.; Mooney, D.J. Metabolic glycan labelling for cancer-targeted therapy. *Nat. Chem.* **2020**, *12*, 1102–1114.
8. Kufleitner, M.; Haiber, L.M.; Wittmann, V. Metabolic glycoengineering—exploring glycosylation with bioorthogonal chemistry. *Chem. Soc. Rev.* **2023**, *52*, 510–535.
9. Ai, X.; Lyu, L.; Zhang, Y.; Rong, J.; Chen, X. Remote regulation of membrane channel activity by site-specific localization of lanthanid-doped upconversion nanocrystals. *Angew. Chem. Int. Ed.* **2017**, *56*, 3031–3035.
10. Agatemor, C.; Buettner, M.J.; Ariss, R.; Muthiah, K.; Saeui, C.T.; Yarema, K.J. Exploiting metabolic glycoengineering to advance healthcare. *Nat. Rev. Chem.* **2019**, *3*, 605–620.
11. Sletten, E.M.; Bertozzi, C.R. Bioorthogonal Chemistry: Fishing for Selectivity in a Sea of Functionality. *Angew. Chem. Int. Ed.* **2009**, *48*, 6974–6998.
12. Hu, M.; Han, Q.; Lyu, L.; Tong, Y.; Dong, S.; Loh, Z.H.; Xing, B. Luminescent molecules towards precise cellular event regulation. *Chem. Commun.* **2020**, *56*, 10231–10234.
13. Droujinine, I.A.; Meyer, A.S.; Wang, D.; Udeshi, N.D.; Hu, Y.; Rocco, D.; Perrimon, N. Proteomics of protein trafficking by in vivo tissue-specific labeling. *Nat. Commun.* **2021**, *12*, 2382.
14. Sampathkumar, S.G.; Li, A.V.; Jones, M.B.; Sun, Z.; Yarema, K.J. Metabolic installation of thiols into sialic acid modulates adhesion and stem cell biology. *Nat. Chem. Biol.* **2006**, *2*, 149–152. https://doi.org/10.1038/nchembio770.
15. Saxon, E.; Bertozzi, C.R. Cell surface engineering by a modified Staudinger reaction. *Science* **2000**, *287*, 2007–2010.
16. Hong, S.; Sahai-Hernandez, P.; Chapla, D.G.; Moremen, K.W.; Traver, D.; Wu, P. Direct Visualization of Live Zebrafish Glycans via Single-Step Metabolic Labeling with Fluorophore-Tagged Nucleotide Sugars. *Angew. Chem. Int. Ed.* **2019**, *58*, 14327–14333.

17. Xie, R.; Hong, S.; Feng, L.; Rong, J.; Chen, X. Cell-selective metabolic glycan labeling based on ligand-targeted liposomes. *J. Am. Chem. Soc.* **2012**, *134*, 9914.
18. Xie, R.; Dong, L.; Huang, R.; Hong, S.; Lei, R.; Chen, X. Targeted imaging and proteomic analysis of tumor-associated glycans in living animals. *Angew. Chem. Int. Ed.* **2014**, *53*, 14082–14086.
19. BDebets, M.F. Metabolic precision labeling enables selective probing of O-linked N-acetylgalactosamine glycosylation. *Proc. Nat. Acad. Sci. USA* **2020**, *117*, 25293–25301.
20. Cioce, A.; Calle, B.; Rizou, T.; Lowery, S.C.; Bridgeman, V.L.; Mahoney, K.E.; Schumann, B. Cell-specific bioorthogonal tagging of glycoproteins. *Nat. Commun.* **2022**, *12*, 6237.
21. Wang, H.; Sobral, M.C.; Zhang, D.K.; Cartwright, A.N.; Li, A.W.; Dellacherie, M.O.; Mooney, D.J. Metabolic labeling and targeted modulation of dendritic cells. *Nat. Mater.* **2020**, *19*, 1244–1252.
22. Wang, H.; Gauthier, M.; Kelly, J.R.; Xu, M.; O'Brien, W.D., Jr.; Cheng, J. Targeted ultrasound-assisted cancer-selective chemical labeling and subsequent cancer imaging using click chemistry. Angewandte Chemie International Edition. *Angew. Chem. Int. Ed.* **2016**, *55*, 5452–5456.
23. Wang, R.; Cai, K.; Wang, H.; Yin, C.; Cheng, J. A caged metabolic precursor for DT-diaphorase- responsive cell labeling. *Chem. Commun.* **2018**, *54*, 4878–4881.
24. Wang, H.; Wang, R.; Cai, K.; He, H.; Liu, Y.; Yen, J.; Cheng, J. selective in vivo metabolic cell-labeling-mediated cancer targeting. *Nat. Chem. Biol.* **2017**, *13*, 415–424.
25. Wang, Z.; Lau, J.W.; Liu, S.; Ren, Z.; Gong, Z.; Liu, X.; Xing, B. A Nitroreductase-Activatable Metabolic Reporter for Covalent Labeling of Pathological Hypoxic Cells in Tumorigenesis. *Angew. Chem. Int. Ed.* **2024**, *136*, e202411636.
26. Shim, M.K.; Yoon, H.Y.; Ryu, J.H.; Koo, H.; Lee, S.; Park, J.H.; Kim, K. Cathepsin B-specific metabolic precursor for in vivo tumor-specific fluorescence imaging. *Angew. Chem. Int. Ed.* **2016**, *55*, 14698–14703.
27. Rillahan, C.D.; Macauley, M.S.; Schwartz, E.; He, Y.; McBride, R.; Arlian, B.M.; Paulson, J.C. Disubstituted sialic acid ligands targeting siglecs CD33 and CD22 associated with myeloid leukaemias and B cell lymphomas. *Chem. Sci.* **2014**, *5*, 2398–2406.
28. Wang, X.; Luo, X.; Tian, Y.; Wu, T.; Weng, J.; Li, Z.; Huang, X. Equipping Natural Killer Cells with Cetuximab through Metabolic Glycoengineering and Bioorthogonal Reaction for Targeted Treatment of KRAS Mutant Colorectal Cancer. *ACS Chem. Biol.* **2012**, *16*, 724–730.
29. Wang, X.; Lang, S.; Tian, Y.; Zhang, J.; Yan, X.; Fang, Z.; Huang, X. Glycoengineering of natural killer cells with CD22 ligands for enhanced anticancer immunotherapy. *ACS Cent. Sci.* **2020**, *6*, 382–389.
30. Han, S.; Collins, B.E.; Bengtson, P.; Paulson, J.C. Homomultimeric complexes of CD22 in B cells revealed by protein-glycan cross-linking. *Nat. Chem. Biol.* **2005**, *1*, 93–97. https://doi.org/10.1038/nchembio713.
31. Lin, B.; Wu, X.; Zhao, H.; Tian, Y.; Han, J.; Liu, J.; Han, S. Redirecting immunity via covalently incorporated immunogenic sialic acid on the tumor cell surface. *Chem. Sci.* **2016**, *7*, 3737.
32. Olson, W.C.; Heston, W.D.; Rajasekaran, A.K. Clinical trials of cancer therapies targeting prostate-specific membrane antigen. *Rev. Recent Clin. Trials* **2007**, *2*, 182–190.
33. Cawley, N.X.; Wetsel, W.C.; Murthy, S.R.K.; Park, J.J.; Pacak, K.; Loh, Y.P. New roles of carboxypeptidase E in endocrine and neural function and cancer. *Endocr. Rev.* **2012**, *33*, 216–153.
34. DiJoseph, J.F.; Dougher, M.M.; Armellino, D.C.; Evans, D.Y.; Damle, N.K. Therapeutic potential of CD22- specific antibody-targeted chemotherapy using inotuzumab ozogamicin (CMC-544) for the treatment of acute lymphoblastic leukemia. *Leukemia* **2007**, *21*, 2240–2245.
35. Kreitman, R.J.; Margulies, I.; Stetler-Stevenson, M.; Wang, Q.C.; FitzGerald, D.J.; Pastan, I. Cytotoxic activity of disulfide-stabilized recombinant immunotoxin RFB4(dsFv)-PE38 (BL22) toward fresh malignant cells from patients with B-cell leukemias. *Clin. Cancer Res.* **2000**, *6*, 1476–1487.
36. Kreitman, R.J.; Wilson, W.H.; Bergeron, K.; Raggio, M.; Stetler-Stevenson, M.; FitzGerald, D.J.; Pastan, I. Efficacy of the anti-CD22 recombinant immunotoxin BL22 in chemotherapy-resistant hairy-cell leukemia. *N. Engl. J. Med.* **2001**, *345*, 241–247.
37. Fry, T.J.; Shah, N.N.; Orentas, R.J.; Stetler-Stevenson, M.; Yuan, C.M.; Ramakrishna, S.; Mackall, C.L. CD22-targeted CAR T cells induce remission in B-ALL that is naive or resistant to CD19-targeted CAR immunotherapy. *Nat. Med.* **2018**, *24*, 20–28.
38. Ramakrishna, S.; Highfill, S.L.; Walsh, Z.; Nguyen, S.M.; Lei, H.; Shern, J.F.; Fry, T.J. Modulation of target antigen density improves CAR T-cell functionality and persistence. *Clin. Cancer Res.* **2019**, *25*, 5329–5341.
39. Zhang, Y.; Gallastegui, N.; Rosenblatt, J.D. Regulatory B cells in anti-tumor immunity. *Int. Immunol.* **2015**, *27*, 521–530.
40. Qin, Y.; Lu, F.; Lyu, K.; Chang, A.E.; Li, Q. Emerging concepts regarding pro-and anti tumor properties of B cells in tumor immunity. *Front. Immunol.* **2022**, *13*, 881427.
41. Sarvaria, A.; Madrigal, J.A.; Saudemont, A. B cell regulation in cancer and anti-tumor immunity. Cellular & molecular immunology. *Cell. Mol. Immunol.* **2017**, *14*, 662–674.

42. Wang, S.S.; Liu, W.; Ly, D.; Xu, H.; Qu, L.; Zhang, L. Tumor-infiltrating B cells: Their role and application in anti-tumor immunity in lung cancer. *Cell. Mol. Immunol.* **2019**, *16*, 6–18.
43. Kinoshita, Y.; Sato, S.; Takeuchi, T. Cellular sialic acid level and phenotypic expression in B16 melanoma cells: Comparison of spontaneous variations and bromodeoxyuridine and theophylline-induced changes. *Cell Struct. Funct.* **1989**, *14*, 35–43.
44. Wieboldt, R.; Sandholzer, M.; Carlini, E.; Lin, C.W.; Börsch, A.; Zingg, A.; Mantuano, N.R. Engagement of sialylated glycans with Siglec receptors on suppressive myeloid cells inhibits anticancer immunity via CCL2. *Cell Mol. Immunol.* **2024**, *21*, 495–509.
45. Kang, J.; Sun, M.; Chang, Y.; Chen, H.; Zhang, J.; Liang, X.; Xiao, T. Butyrate ameliorates colorectal cancer through regulating intestinal microecological disorders. *Anti-Cancer Drugs* **2023**, *34*, 227–237.
46. Li, Y.; He, P.; Chen, Y.; Hu, J.; Deng, B.; Liu, C.; Dong, W. Microbial metabolite sodium butyrate enhances the anti-tumor efficacy of 5-fluorouracil against colorectal cancer by modulating PINK1/Parkin signaling and intestinal flora. *Sci. Rep.* **2024**, *14*, 13063.
47. Archer, S.Y.; Meng, S.; Shei, A.; Hodin, R.A. p21WAF1 is required for butyrate-mediated growth inhibition of human colon cancer cells. *Proc. Natl. Acad. Sci. USA* **1998**, *95*, 6791–6796.
48. Kruh, J. Effects of sodium butyrate, a new pharmacological agent, on cells in culture. *Mol. Cell Biochem.* **1981**, *42*, 65–82.
49. Chen, W.C.; Completo, G.C.; Sigal, D.S.; Crocker, P.R.; Saven, A.; Paulson, J.C. In vivo targeting of B-cell lymphoma with glycan ligands of CD22. *Blood* **2010**, *115*, 4778–4786.
50. Zaccai, N.R.; Maenaka, K.; Maenaka, T.; Crocker, P.R.; Brossmer, R.; Kelm, S.; Jones, E.Y. Structure-guided design of sialic acid-based Siglec inhibitors and crystallographic analysis in complex with sialoadhesin. *Structure* **2003**, *11*, 557–567.
51. Kelm, S.; Gerlach, J.; Brossmer, R.; Danzer, C.P.; Nitschke, L. The ligand-binding domain of CD22 is needed for inhibition of the B cell receptor signal, as demonstrated by a novel human CD22-specific inhibitor compound. *J. Exp. Med.* **2002**, *195*, 1207–1213.
52. Büll, C.; Boltje, T.J.; Wassink, M.; de Graaf, A.M.; van Delft, F.L.; den Brok, M.H.; Adema, G.J. Targeting aberrant sialylation in cancer cells using a fluorinated sialic acid analog impairs adhesion, migration, and in vivo tumor growth. Molecular cancer therapeutics. *Mol. Cancer Ther.* **2013**, *12*, 1935–1946.
53. Rodrigues, E.; Macauley, M. Hypersialylation in Cancer: Modulation of Inflammation and Therapeutic Opportunities. *Cancers* **2018**, *10*, 207.
54. Pearce, O.M.; Läubli, H. Sialic acids in cancer biology and immunity. *Glycobiology* **2015**, *26*, 111–128.
55. Hudak, J.E.; Canham, S.M.; Bertozzi, C.R. Glycocalyx engineering reveals a Siglec-based mechanism for NK cell immunoevasion. *Nat. Chem. Biol.* **2014**, *10*, 69–75.
56. O'Reilly, M.K.; Paulson, J.C. Siglecs as targets for therapy in immune-cell-mediated disease. Trends in pharmacological sciences. *Trends Pharmacol. Sci.* **2009**, *30*, 240–248.
57. Jakobsche, C.E.; Parker, C.G.; Tao, R.N.; Kolesnikova, M.D.; Douglass, E.F., Jr.; Spiegel, D.A. Exploring binding and effector functions of natural human antibodies using synthetic immunomodulators. *ACS Chem. Biol.* **2013**, *8*, 2404–2411. https://doi.org/10.1021/cb4004942.
58. Murelli, R.P.; Zhang, A.X.; Michel, J.; Jorgensen, W.L.; Spiegel, D.A. Chemical control over immune recognition: A class of antibody-recruiting small molecules that target prostate cancer. *J. Am. Chem. Soc.* **2009**, *131*, 17090–17092. https://doi.org/10.1021/ja906844e.
59. Parker, C.G.; Domaoal, R.A.; Anderson, K.S.; Spiegel, D.A. An antibody-recruiting small molecule that targets HIV gp120. *J. Am. Chem. Soc.* **2009**, *131*, 16392–16394. https://doi.org/10.1021/ja9057647.
60. Fura, J.M.; Sabulski, M.J.; Pires, M.M. D-amino acid mediated recruitment of endogenous antibodies to bacterial surfaces. *ACS Chem. Biol.* **2014**, *9*, 1480–1489. https://doi.org/10.1021/cb5002685.
61. Cheadle, E.J.; Gornall, H.; Baldan, V.; Hanson, V.; Hawkins, R.E.; Gilham, D.E. CAR T cells: Driving the road from the laboratory to the clinic. *Immunol. Rev.* **2014**, *257*, 91–106. https://doi.org/10.1111/imr.12126.
62. Tomayko, M.M.; Reynolds, C.P. Determination of subcutaneous tumor size in athymic (nude) mice. *Cancer Chemother. Pharmacol.* **1989**, *24*, 148–154.